

Effect of La, Zr Doping on the Structural and Electrical Conduction Behaviour of BiFeO₃-BaTiO₃ Ceramics

Siddharth Pratap Singh¹, Amar Bahadur Verma¹, Ankur Srivastava¹, Pravesh Kumar Vishwakarma¹, Anil Kumar¹, Prashant Kumar Singh², Sindhu Singh¹

¹Material Synthesis Laboratory, Department of Physics and Electronics, Dr. Rammanohar Lohia Avadh University, Ayodhya, Uttar Pradesh, India

²Department of Applied Sciences and Humanities, Institute of Engineering and Technology, Dr. Rammanohar Lohia Avadh University, Ayodhya, Uttar Pradesh, India
sindhusingh@rmlau.ac.in¹

ARTICLE INFO

Article History:

Accepted: 10 Feb 2024

Published: 24 Feb 2024

Publication Issue :

Volume 11, Issue 1

January-February-2024

Page Number :

520-525

ABSTRACT

This study presents a comprehensive investigation of the crystal structure and DC conduction mechanism of [(Ba_{0.7-x} La_x) Bi_{0.3}][(Ti_{0.5} Zr_{0.2}) Fe_{0.3}]O₃ with x = 0.00, 0.01, 0.03, 0.05 employing X-ray diffraction (XRD) and electrical conductivity measurements. Various compositions were synthesized through the solid-state ceramic route. XRD was used to investigate phase formation. Analysis of XRD data suggested a structural transition from cubic to tetragonal for x ≥ 0.01. The average crystallite size first increases for x = 0.01 and then decreases for x ≥ 0.03. The temperature-dependent electrical conductivity measurements were investigated over a wide temperature range which revealed distinct conductivity mechanisms governing the material's transport properties. The activation energy (E_a) has been estimated from temperature-dependent DC conductivity. Overall, this study provides valuable insights into the correlation between crystal structure and electrical properties in [(Ba_{0.7-x} La_x) Bi_{0.3}][(Ti_{0.5} Zr_{0.2}) Fe_{0.3}]O₃, offering significant implications for its potential applications in electronic and optoelectronic devices requiring tailored conductivity characteristics.

Keywords: Multiferroic, Solid-State route, XRD, DC conductivity

I. INTRODUCTION

Multiferroics are materials that show more than one fundamental ferroic properties simultaneously (i.e., in a single phase) [1] while many researchers in the field consider materials to be multiferroics only if they

exhibit coupling between ferroelectric and magnetic orders. Multiferroic materials have become an important research field to be studied extensively because of their physical properties like ferroelectric, ferromagnetic, and ferroelastic [2], [3]. The application capabilities of multiferroics depend

mainly on the degree of coupling between specific subsystems (magnetic, electric, or elastic) and varied multifunctional device applications such as multiple-state memory, sensors, multilayer capacitors, actuators, electro-optic, and acoustic-optic devices[4], [5]. Ferroelectricity occurs in material with empty d-orbitals whereas ferromagnetism occurs in partially filled d or f orbitals[6]. Composites of ferroelectric and ferromagnetic materials are important for developing magnetoelectronic devices in distinct frequency regions. BiFeO₃ (BFO) is a favorable material having a perovskite structure and can be produced at ambient temperature where ferromagnetism and anti-ferromagnetism coexist. The material has amazing potential under a ferroelectric Curie temperature (T_C) (830°C) and an antiferroelectric Neel temperature (T_N)(370°C)[3]. Pure BiFeO₃ ceramics are difficult to crystallize by high insulation methods because during sintering Bi evaporates and Fe³⁺ ions change to Fe²⁺ ions. In BFO due to the presence of Fe²⁺ ions and oxygen deficiency along with structural deformation, it is difficult to get improved ferroelectric properties. This also causes some other problems such as lower resistivity and a high value of leakage current in BFO[7]. Consequently, BFO multiferroic exhibits less spontaneous polarisations, high dielectric loss, and low dielectric constant at 27°C. Rare earth elements like (La, Ce, Sm, and Gd) have also been used for the improvements of these multifunctional materials on the A/B site as well as other ABO₃-type perovskite materials[8][9]. According to researchers, replacing (Bi ions) from the A-site and (Fe ions) from the B-site in BFO-based ceramics with rare earth ions and reducing the value of leakage current through transition metal ions develops piezoelectric activity[10][11].

BaTiO₃ (BTO) is a piezoelectric material with giant polarisation because of shifting of Ti⁴⁺ off from the centrosymmetric position into the TiO₆ octahedra[12]. It exhibits a Positive Temperature Coefficient of Resistance (PTCR) when low impurities of higher valence state are added at A and B sites. It is

mentioned that addition of Bi³⁺ at the Ba²⁺ site exhibits PTCR [13]but the inclusion of Fe³⁺ causes it to display semiconducting behavior[14].

In the best of our knowledge no work is reported on La, Zr modified BFO-BTO ceramic compounds in the literature. In the present paper, we are reporting preparation, structural and electrical conduction mechanism of [(Ba_{0.7-x} La_x) Bi_{0.3}][(Ti_{0.5} Zr_{0.2}) Fe_{0.3}]O₃ (x = 0.00, 0.01, 0.03, 0.05).

II. EXPERIMENTAL DETAILS

La-substituted ceramics were synthesized based on the chemical formula of [(Ba_{0.7-x} La_x) Bi_{0.3}][(Ti_{0.7-y} Zr_y)Fe_{0.3}]O₃ (x = 0.00, 0.01, 0.03, 0.05) using conventional solid-state ceramic route at high temperature. Bi₂O₃ (99%, Fisher Scientific), Fe₂O₃ (100%, Sigma Aldrich), BaCO₃ (99%, Himedia), TiO₂ (98%, Loma Chemie), ZrO₂ (99.9%, Otto), La₂O₃ (99.9%, Sigma Aldrich), C₂H₂O₄ (99%, Fisher Scientific) were used as raw materials. Since lanthanum oxide (La₂O₃) is hygroscopic, it is impossible to weigh it accurately. Therefore, replacing this compound with another non-hygroscopic compound is advisable, which can finally yield La₂O₃. We have used Lanthanum oxalate for this purpose.

Raw materials were weighed as per the stoichiometric ratios, then mixed and milled for 6 h using acetone and zirconia media in a roller ball mill to obtain homogenous mixtures. The homogenized mixtures were dried overnight to evaporate all the acetone. Then, the obtained powder was crushed and calcined progressively in alumina crucibles at 900°C/10h, and 1000°C/10h in air with an intermediate regrinding to enhance the purity of obtained products. The slow rates of heating and cooling were 3°C/ min for each heat treatment. Afterward, a small amount of 2% polyvinyl alcohol (PVA used as a binder) dissociated in water was added and mixed with the resulting powders of different compositions. The mixed powders were pressed as cylindrical pellets having a thickness in the range of 1-2 mm and a diameter of 12

mm in a Hydraulic Press under an optimum load of 60 N/m². Thereafter, pellets were kept in furnace and its temperature was raised at a rate of 3°C/ min to the sintering temperature 1050°C/ 10h. The obtained pellets were cooled progressively to room temperature (RT), providing structural, and electrical measurements on the sintered pellets. Phase check and formation of the structure for the compounds were carried out using an X-ray powder diffractometer, the PANalytical X'Pert Pro, with CuK α radiation (wavelength (λ) = 1.5405 Å) at RT. Scanning rate was kept at 2°/ min over a broad range for 2 θ (20° < 2 θ < 60°).

The DC electrical conductivity was assessed in the temperature range of 27 - 447°C using a Keithley 224 electrometer.

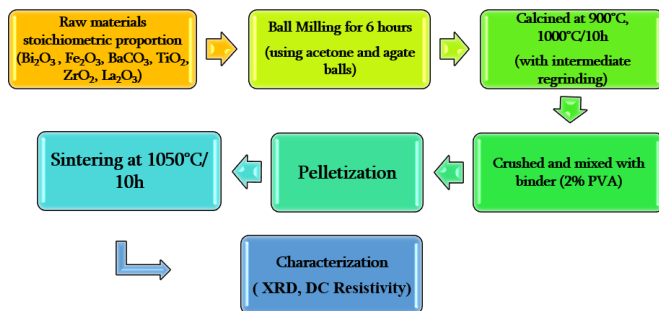


Fig 1: Flowchart for synthesis of material

III. RESULTS AND DISCUSSION

A. XRD analysis

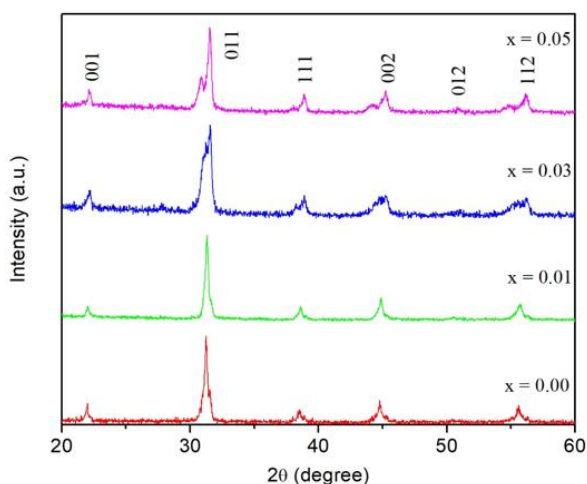


Fig. 2: XRD diagram of La, Zr doped BiFeO₃ – BaTiO₃ compounds.

Fig 2. represents the XRD of La and Zr doped BiFeO₃-BaTiO₃ prepared samples in the 2 θ range of 20° to 60° at RT. The XRD pattern for all the compositions matches with pure perovskite structure without any impurity phases within the measured range of 2 θ angle. All the peaks recorded were refined by the least square fitting through the software 'EXPO2014'. The obtained diffraction peaks are (001), (011), (111), (002), (012), and (112) correspond to the angles 22.03°, 31.31°, 38.61°, 44.92°, and 55.71°. For x = 0.00 and x = 0.01 no splitting in peak positions on the reflection plane (011) indicates the formation of cubic structure while clear splitting is observed for x = 0.03, 0.05

$$D = \frac{k\lambda}{\beta \cos\theta} \quad (1)$$

compositions indicate formation of tetragonal structure. Similar results were also reported by Kar et al[10] where they obtained the tetragonal phase for the 0.56Bi_{1-x}La_xFeO₃-0.44BaTiO₃ with x = 0 to 0.20. Previous studies reported the tetragonal crystal symmetry for 0.65BFO-0.35BTO to 0.55BFO-0.45BTO[15]. The obtained lattice parameter (LP) reveals that on increasing the doping percentage structure changes from cubic to tetragonal phase. The change in both LP and cell volume can be explained by the partial substitution of Fe²⁺ (0.77Å) ions and Fe³⁺ (0.63Å) ions. The variations in the LP are because of the existence of multivalent Fe ions in the mother material. The calculated values for lattice parameters and volume of cells for all the compositions are given in Table 1. The large LP for x=0.03 suggests that more Fe²⁺ ions are present than Fe³⁺ ions.

Crystallite size (D) was calculated using the Debye-Scherrer equation[16][17]:

where K = 0.9 or 1 is the structure factor for the cubic system, $\lambda = 1.54\text{Å}$ represents a wavelength of Cu-K α radiation, β represents full-width half maxima (FWHM), θ denotes Bragg's angle. β and θ both are taken in radians.

The average crystallite size values for each composition vary from 523.22 nm ~ 349.25 nm. Dislocation in the samples was calculated using the following formula[18]:

$$\delta = \frac{1}{D^2} \tag{2}$$

where D represents crystallite size calculated through the Scherrer formula.

Dislocation densities were calculated from average crystallite size obtained from the Scherrer method using (Eq. (2)). Variations in dislocation densities were found from 0.0000036 nm⁻² to 0.0000081 nm⁻² as given in Table 1. For the A_{1-x}A'_xB_{1-x}B'_xO₃ type complex perovskite oxides, formation of a single perovskite phase, structure stability, and structural distortion of the perovskite phase can be determined using the tolerance factor (t) which is expressed by Goldschmidt relation as given below[19]:

$$t = \frac{R_{O^{2-}} + xR_{Bi^{3+}} + (1-x)R_{La^{2+}} + (1-x)R_{Ba^{2+}}}{\sqrt{2((1-x)R_{Ti^{4+}} + xR_{Fe^{3+}} + (1-x)R_{Zr^{4+}} + R_{O^{2-}})}} \tag{3}$$

where, R_{Ba²⁺}, R_{La²⁺}, R_{Bi³⁺}, R_{Fe³⁺}, R_{Ti⁴⁺}, R_{Zr⁴⁺} are the ionic radii of Ba²⁺, La²⁺, Bi³⁺, Fe³⁺, Ti⁴⁺, and Zr⁴⁺ cations respectively. R_{O²⁻} represents the ionic radius of oxygen anion O²⁻. Eq. 3 has been used to calculate the tolerance factor. The ionic radii used to calculate the tolerance factor were taken over from the Shannon table[20]. The values of the tolerance factor increased for x = 0.01, whereas on increasing the La content it decreased. This might be due to the smaller ionic radii of the La²⁺ (1.06Å) dopant compared to the ionic radii of Ba²⁺ (1.36Å).

Volume (Å ³)	65.80	66	506	329
Structure	Cubic	Tetragonal	Tetragonal	Tetragonal
Space Group (SG)	Pm-3m	P4/mmm	P4/mmm	P4/mmm
Crystallite Size (D) (nm)	523.22	697.10	418.51	349.25
Tolerance Factor (τ)	0.912	0.98	0.978	0.977
Dislocation Density (δ) (nm ⁻²)	0.0000036 36	0.0000002 2	0.0000057 57	0.0000081 81

A. Electrical conduction mechanism

Plots of the logarithm of DC conductivity, log σ_{dc} (ohm-cm)⁻¹ versus 1000/T (K)⁻¹ are demonstrated in Fig 3. For all the compositions, conductivity increases with increasing temperature which indicates its insulating behavior. There are two slope changes in the temperature region 27- 447°C. Conductivity in these regions obeys the Arrhenius relationship[21] according to the equation

$$\sigma_{dc} = \sigma_0 \exp\left(-\frac{E_a}{k_B T}\right) \tag{4}$$

Where E_a denotes the activation energy for conduction. Contrary to the case of doped BaTiO₃ no PTCR effect is seen. A low resistivity value at RT was observed when compared with pure BaTiO₃. The change in slope at 97°C may be owing to dielectric transition. Modification with La, Zr has increased room temperature DC conductivity from 1.62402 X 10⁻⁹ Ωcm⁻¹ to 4.28535 X 10⁻⁹ Ωcm⁻¹ for x = 0.00-0.05. This can be because of increased grain boundary resistivity. Values of activation energies in various temperature ranges attained by the least square data fitting are given in Table 2. As the doping concentration of La i.e., x increases the value of E_a decreases. For each composition, the activation

Parameter	0%	0.01%	0.03%	0.05%	
Lattice constants (Å)	a	4.03716	4.03958	4.72836	4.09430
	c	5	3	2	8
		4.03039	22.6389	19.6265	
		7	64	45	

energy is greater in the higher temperature region than lower temperature region. The first slope may be attributed to impurity conduction.

Table 2: Activation energy, E_a for DC conduction in the system $\{(Ba_{0.7-x}La_x)Bi_{0.3}\}\{(Ti_{0.7-y}Zr_y)Fe_{0.3}\}O_3$		
Composition	Temperature range (°C)	E_a (eV)
x = 0.00	136°C - 202°C	0.54
	212°C - 400°C	1.11
x = 0.01	102°C - 232°C	0.59
	237°C - 447°C	0.70
x = 0.03	67°C - 157°C	0.52
	172°C - 447°C	0.66
x = 0.05	62°C - 222°C	0.55
	227°C - 447°C	0.63

IV. CONCLUSION

La, Zr doped BiFeO₃- BaTiO₃ material has been synthesized through a low-cost conventional solid-state ceramic route. The cubic to tetragonal phase transition with an increase in the doping percentage of La has been observed through XRD analysis. In BiFeO₃-BaTiO₃ ceramics, the substitution of La and Zr has shown stabilization in the crystal structure and increased the sample density. The E_a of the conduction decreased with increasing x due to availability of more charge carriers.

V. ACKNOWLEDGMENT

This work was funded by the Uttar Pradesh government under the Research and Development scheme Grant no. -80/2021/1543/sattar-4-2021-4(28)/2021.

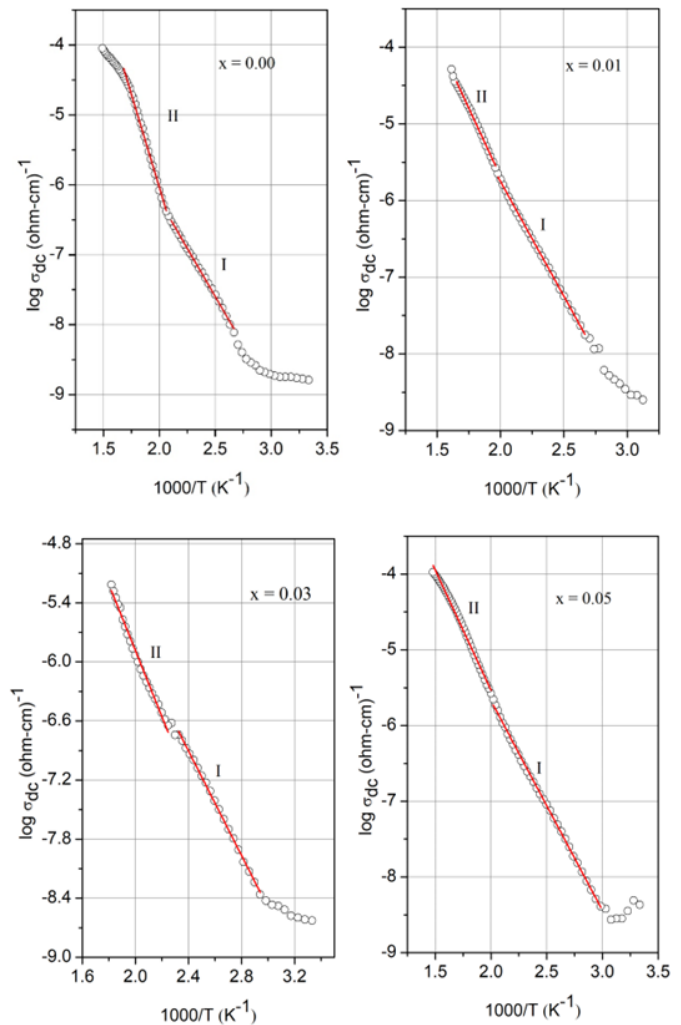


Fig 3 : Graph of Temperature-dependent DC conductivity for all the compositions

VI. REFERENCES

- [1]. V. A. Khomchenko et al., "Effect of Gd substitution on the crystal structure and multiferroic properties of BiFeO₃," *Acta Mater.*, vol. 57, no. 17, pp. 5137–5145, 2009.
- [2]. M. P. K. Sahoo, Z. Yajun, J. Wang, and R. N. P. Choudhary, "Composition control of magnetoelectric relaxor behavior in multiferroic BaZr_{0.4}Ti_{0.6}O₃/CoFe₂O₄ composites," *J. Alloys Compd.*, vol. 657, pp. 12–20, 2016.
- [3]. J. Wang et al., "Epitaxial BiFeO₃ multiferroic thin film heterostructures," *Science* (80-.), vol. 299, no. 5613, pp. 1719–1722.
- [4]. N. Hur, S. Park, P. A. Sharma, J. S. Ahn, S. Guha, and S. W. Cheong, "Electric polarization reversal

- and memory in a multiferroic material induced by magnetic fields,” *Nature*, vol. 429, no. 6990, pp. 392–395.
- [5]. W. Prellier, M. P. Singh, and P. Murugavel, “The single-phase multiferroic oxides: From bulk to thin film,” *J. Phys. Condens. Matter*, vol. 17, no. 30, 2005.
- [6]. A. C. Turnock and H. P. Eugster, “Fe - Al Oxides: Phase relationships below 1,000C1,” *J. Petrol.*, vol. 3, no. 3, pp. 533–565, 1962.
- [7]. M. Rawat and K. L. Yadav, “Study of structural, electrical, magnetic and optical properties of 0.65BaTiO₃-0.35Bi_{0.5}Na_{0.5}TiO₃-BiFeO₃ multiferroic composite,” *J. Alloys Compd.*, vol. 597, pp. 188–199, 2014.
- [8]. Y. Zhang et al., “Enhancement of piezoelectric properties of BF–BT ceramics by using ZrO₂ powder bed during the sintering process,” *J. Am. Ceram. Soc.*, no. November 2022, pp. 2384–2392, 2022.
- [9]. Q. Zhang et al., “Effect of La³⁺ substitution on the phase transitions, microstructure and electrical properties of Bi_{1-x}La_xFeO₃ ceramics,” *J. Alloys Compd.*, vol. 546, pp. 57–62, 2013.
- [10]. B. S. Kar, M. N. Goswami, and P. C. Jana, “Effects of lanthanum dopants on dielectric and multiferroic properties of BiFeO₃–BaTiO₃ ceramics,” *J. Alloys Compd.*, vol. 861, p. 157960, 2021.
- [11]. S. S. Chowdhury et al., “Dy doped BiFeO₃: A bulk ceramic with improved multiferroic properties compared to nano counterparts,” *Ceram. Int.*, vol. 43, no. 12, pp. 9191–9199, 2017.
- [12]. C. Lan, Y. Jiang, and S. Yang, “Magnetic properties of La and (La, Zr) doped BiFeO₃ ceramics,” *J. Mater. Sci.*, vol. 46, no. 3, pp. 734–738, 2011.
- [13]. O. Saburi, “Properties of Semiconductive Barium Titanates,” *Journal of the Physical Society of Japan*, vol. 14, no. 9, pp. 1159–1174.
- [14]. M. Mahesh Kumar, M. B. Suresh, S. V. Suryanarayana, G. S. Kumar, and T. Bhimasankaram, “Dielectric relaxation in Ba_{0.96}Bi_{0.04}Ti_{0.96}Fe_{0.04}O₃,” *J. Appl. Phys.*, vol. 84, no. 12, pp. 6811–6814, 1998.
- [15]. Y. Wei, J. Zhu, X. Wang, J. Jia, and X. Wang, “Dielectric, ferroelectric, and piezoelectric properties of BiFeO₃-BaTiO₃ ceramics,” *J. Am. Ceram. Soc.*, vol. 96, no. 10, pp. 3163–3168, 2013.
- [16]. K. M. Batoo et al., “Improved room temperature dielectric properties of Gd³⁺ and Nb⁵⁺ co-doped Barium Titanate ceramics,” *J. Alloys Compd.*, vol. 883, p. 160836, 2021.
- [17]. M. K. Anupama, B. Rudraswamy, and N. Dhananjaya, “Investigation on impedance response and dielectric relaxation of Ni-Zn ferrites prepared by self-combustion technique,” *J. Alloys Compd.*, vol. 706, pp. 554–561, 2017.
- [18]. K. M. Batoo et al., “Structural, morphological and electrical properties of Cd²⁺-doped MgFe₂-xO₄ ferrite nanoparticles,” *J. Alloys Compd.*, vol. 726, pp. 179–186, 2017.
- [19]. Z. Chchiyai et al., “Design, structural evolution, optical, electrical and dielectric properties of perovskite ceramics Ba_{1-x}BixTi_{1-x}FexO₃ (0 ≤ x ≤ 0.8),” *Mater. Chem. Phys.*, vol. 273, no. June, 2021.
- [20]. R. D. Shannon and C. T. Prewitt, “Revised values of effective ionic radii,” *Acta Crystallogr. Sect. B Struct. Crystallogr. Cryst. Chem.*, vol. 26, no. 7, pp. 1046–1048, 1970.
- [21]. P. Singh, P. Singh, S. Singh, O. Parkash, and D. Kumar, “Electrical conduction behavior and immittance analysis of Gd and Mn substituted strontium titanate,” *J. Mater. Sci.*, vol. 43, no. 3, pp. 989–1001, 2008.

Cite this article as :

Siddharth Pratap Singh, Amar Bahadur Verma, Ankur Srivastava, Pravesh Kumar Vishwakarma, Anil Kumar, Prashant Kumar Singh², Sindhu Singh, "Effect of La, Zr Doping on the Structural and Electrical Conduction Behaviour of BiFeO₃-BaTiO₃ Ceramics", *International Journal of Scientific Research in Science and Technology (IJSRST)*, Online ISSN : 2395-602X, Print ISSN : 2395-6011, Volume 11 Issue 1, pp. 520-525, January-February 2024. Available at doi : <https://doi.org/10.32628/IJSRST52411180>
Journal URL : <https://ijsrst.com/IJSRST52411180>